Hybrid Power Quality Compensator With Minimum DC Operation Voltage Design for High-Speed Traction Power Systems

Keng-Weng Lao, *Student Member, IEEE*, NingYi Dai, *Member, IEEE*, Wei-Gang Liu, and Man-Chung Wong, *Senior Member, IEEE*

Abstract—**A hybrid power quality compensator (HPQC) is proposed in this paper for comprehensive compensation under minimum dc operation voltage in high-speed traction power supplies. Reduction in HPQC operation voltage can lead to a decrease in the compensation device capacity, power consumptions, and installation cost. The parameter design procedures for minimum dc voltage operation of HPQC are being explored. It is shown through simulation results that similar compensation performances can be provided by the proposed HPQC with reduced dc-link voltage level compared to the conventional railway power compensator. The system rating can thus be reduced. It is also verified that HPQC would operate at the minimum dc voltage with the proposed parameter design via simulations. A hardware prototype is constructed and the experimental results show that through the proposed design, HPQC is able to provide system unbalance, reactive power, and harmonic compensation in cophase traction power with reduced operation voltage. The cophase traction power supply with proposed HPQC is suitable for high-speed traction applications.**

Index Terms—**Cophase system, power quality compensator, reactive power compensation, traction power, unbalance compensation.**

I. INTRODUCTION

TRACTION power supply systems usually suffer from different power quality problems [1]–[3]. One of the widely applied modes is the single-phase voltage electrified traction load. Due to the fact that traction loads are dynamic and time varying, huge amount of negative sequence current is injected into the three-phase power grid, causing undesired system unbalance. In addition, applications of nonlinear power electronics converters in locomotives also inject significant amount of harmonics into the system. Existence of harmonics and system unbalance in the power system may generate undesired heat loss and cause damage to the system [4]. In addition, due to the fact that most locomotive loadings are inductive, the system may possess reactive power. The presence of reactive power in the power system may indicate inefficient usage of the apparent power supplied by the system [5]. With increasing usage of novel technologies in traction loads, the problems may become more severe [6].

Various techniques have been proposed to solve the system unbalance problem in traction power supply. When balanced transformers such as Scott and roof-delta transformers are used, the system unbalance problem can be relieved [7]–[9]. However, with varying traction loads, the system can hardly be completely balanced. Moreover, the technique usually involves construction of special transformers, which add to the total installation cost. In addition, there is no help against the problem of reactive power and harmonics. Compared to passive compensators, active compensators can provide better dynamic and comprehensive compensation. Railway power compensator (RPC) was thus proposed as a universal compensation device which can provide fast and dynamic unbalance, reactive power and harmonics compensation in traction power [10], [11].

Cophase traction power supply system is one of the newly proposed traction power systems which solve the problem of excessive neutral sections installation in traction power supplies [12]–[14]. Elimination of neutral sections may reduce the velocity loss of the locomotives, and cophase traction power thus has high potential as high-speed traction power supply system. Locomotive loads are connected across the same single-phase output to avoid risk of phase mixing. The compensation device (such as RPC) is then connected into the system to provide system power quality compensation. Various RPCs have been proposed for cophase traction power systems [15]–[18]. However, the popularity of cophase traction power is prohibited by the high operation voltage of the compensation device. The initial cost of passive compensation device is only USD$5/kVA while that of active compensation device is around USD $60/kVA [19]. It would be advantageous if active compensators can be combined with passive ones during compensation [20]. Different pieces of research have been done on usage and design of hybrid filter [21]–[23]. However, there is still lack of research on the application and parameter design of hybrid structure in the power compensator for the cophase traction power supply system. For instance, in cophase traction power involving V/V transformer, active power injection is required for system unbalance compensation. This makes the analysis and design different from the traditional hybrid filter.

In this paper, a hybrid device combining active and passive compensators, named as the hybrid power quality compensator

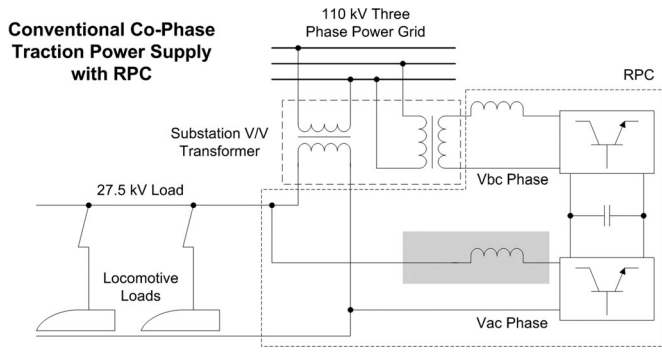Fig. 1. Circuit configuration of the conventional cophase traction power supply system with RPC.

Fig. 2. Circuit configuration of the proposed cophase traction power supply with HPQC.

(HPQC), is proposed for compensation in cophase traction power supply. The parameter design procedure for minimum HPQC voltage operation as well as the minimum voltage rating achievable is discussed. Descriptions of proposed circuit configurations of cophase traction power with HPQC are provided in Section II, together with comparisons with conventional RPC. The parameter design for the minimum HPQC voltage operation and the minimum operation voltage achievable is investigated in Section III. Control philosophy of the system is presented in Section IV. Simulation verifications are given in Section V concerning HPQC compensation performances under minimum operation dc voltage, as well as its comparisons with conventional RPC. Hardware descriptions and experimental results are then presented in Section VI. Finally, the research targets and major contributions are concluded in Section VII.

II. CONVENTIONAL AND PROPOSED SYSTEM CIRCUIT CONFIGURATIONS

The circuit configuration of the conventional cophase traction power supply with RPC is given in Fig. 1. In this project, the substation transformer is composed of two single-phase transformers, and is commonly known as the V/V transformer. The three-phase power grid is transformed into two single-phase outputs (V_{ac} and V_{bc} phases) through V/V transformer. The locomotive loadings are all connected across the same single-phase output (V_{ac}), leaving another phase (V_{bc}) unloaded. The RPC is composed of one back-to-back converter and is connected across the V_{ac} and V_{bc} phases, so as to provide power quality compensation for the system.

The circuit configuration of the proposed cophase traction power supply with HPQC is shown in Fig. 2. In contrast to conventional structure, the converter is connected to the V_{ac} phase of the transformer via a capacitive coupled hybrid *LC* structure. As will be discussed later, this results in the reduction of converter dc bus voltage of HPQC.

The compensation algorithm of the proposed HPQC is similar to that in conventional RPC and is not discussed here. Details may be found in [16] and [19]. For better understanding of the discussions, the detailed structure and physical definitions of RPC in the conventional structure and HPQC in the proposed structure are presented in Fig. 3.
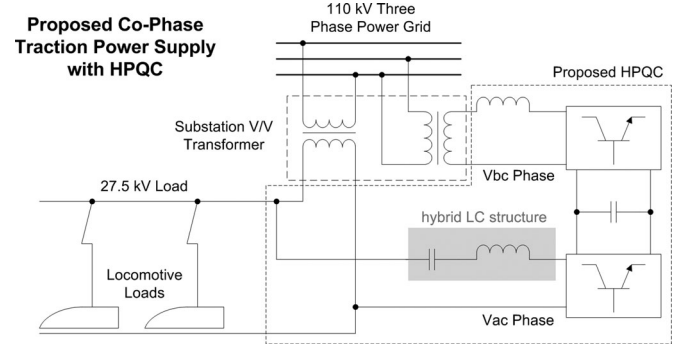
Since traction loads are mostly inductive, the following contents are discussed based on the assumption of inductive loadings. The vector diagrams of the V_{ac} phase converter for the conventional RPC and proposed HPQC are shown in Fig. 4.

It can be observed that with capacitive coupled *LC* structure, the amplitude of $V_{\mathrm{inva}LC}$ in HPQC can be less than that of $V_{\mathrm{inva}L}$ in RPC under the same compensation current. The corresponding mathematical expressions are shown in (1) and (2). With capacitive coupled structure in HPQC, X_{LCa} is of negative value, and it results in reduction of $V_{\mathrm{inva}LC}$. Details of compensation current in cophase traction power may be found in [19]

$$|V_{\mathrm{inva}L}| = \sqrt{V_{\mathrm{inva}Lp}^2 + V_{\mathrm{inva}Lq}^2}$$
$$= \sqrt{(V_{ac} + |I_{caq}| X_{La})^2 + (|I_{cap}| X_{La})^2} \quad (1)$$
$$|V_{\mathrm{inva}LC}| = \sqrt{V_{\mathrm{inva}LCp}^2 + V_{\mathrm{inva}LCq}^2}$$
$$= \sqrt{(V_{ac} + |I_{caq}| X_{LCa})^2 + (|I_{cap}| X_{LCa})^2} \quad (2)$$

where $|I_{caq}| = I_L \left[\frac{1}{2\sqrt{3}} (\mathrm{PF}) + \sin\left(\cos^{-1}(\mathrm{PF})\right) \right]$ and $|I_{cap}| = I_L \left(\frac{1}{2\mathrm{PF}} \right)$.

Based on (1) and (2), it can be concluded that with fixed value of V_{ac}, the values of $V_{\mathrm{inva}L}$ and $V_{\mathrm{inva}LC}$ are highly dependent on the V_{ac} phase coupled impedance. The 3-D plots showing the variation of $V_{\mathrm{inva}L}$ and $V_{\mathrm{inva}LC}$ with V_{ac} phase coupled impedance under different load power factor (PF) for RPC and HPQC are shown in Fig. 5.

It can be observed that the $V_{\mathrm{inva}L}$ rating in RPC of the conventional structure increases linearly with the V_{ac} coupled impedance, and the value of $V_{\mathrm{inva}L}/V_{ac}$ is always larger than 1.0, which indicates that the required amplitude of $V_{\mathrm{inva}L}$ is higher than that of V_{ac}. In contrast, $V_{\mathrm{inva}LC}$ in HPQC of the proposed structure is a U- or V-shaped surface, possessing specific minimum voltage operating points. Different from that in RPC, the value can be less than 1.0, indicating that the required amplitude of $V_{\mathrm{inva}LC}$ can be less than that of V_{ac}.

For example, the PF of traction loads normally ranges from 0.8 to 0.85 [24]. The variations of $V_{\mathrm{inva}LC}$ voltage rating with
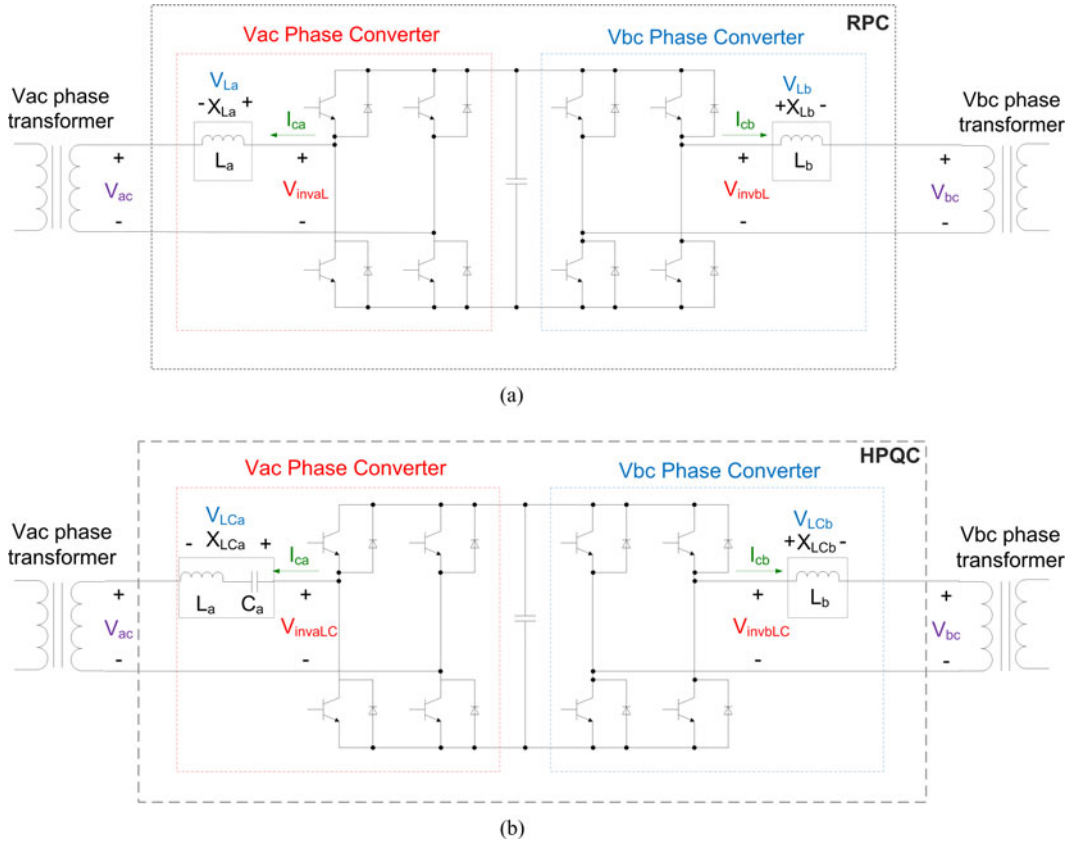
Fig. 3.   Detailed structure and physical definitions of (a) RPC in the conventional cophase traction power and (b) HPQC in the proposed cophase traction power.
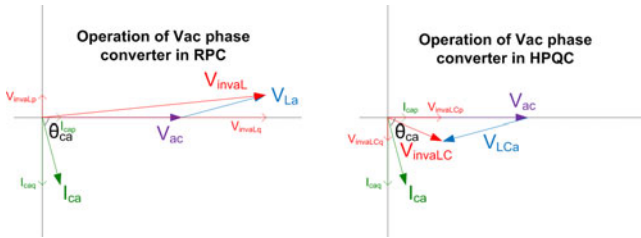

Fig. 4.   Vector diagram showing the operation of V_{ac} phase converter in (a) RPC of the conventional structure and (b) HPQC of the proposed structure.

V_{ac} coupled impedance in RPC and HPQC under load PF of 0.85 are shown graphically in Fig. 6.

The figure shows clearly that under the examined condition, the value of $V_{\mathrm{inva}L}$ in RPC is higher than that of $V_{\mathrm{inva}LC}$ in HPQC. Moreover, there is a minimum voltage operation point for HPQC. For instance, with load PF of 0.85, the minimum value of $V_{\mathrm{inva}LC}$ in HPQC is approximately 48% of V_{ac} phase voltage. The operation point can be tuned along the curve by changing the V_{ac} coupled impedance. Therefore, the HPQC operation could be located at the minimum voltage operation point via specific parameter design. The detailed discussions are given in the next section.

III. HPQC Parameter Design for the Minimum DC Voltage Operation

The parameter design for the minimum dc voltage operation of HPQC in the proposed structure is being explored in this section. The design procedures of V_{ac} and V_{bc} phase coupled impedance are introduced, together with the investigations on the minimum HPQC dc voltage rating achievable.

A. V_{ac} Phase Coupled Impedance Design

The vector diagram showing the operation of V_{ac} phase converter in HPQC under minimum voltage operation is given in Fig. 7. With constant load PF and capacity, the vector I_{ca} is fixed. Thus, the vector V_{LCa} would vary along the line L_1 as the V_{ac} coupled impedance X_{LCa} varies. It can be observed that the amplitude of $V_{\mathrm{inva}LC}$ can be minimized when it is perpendicular to the vector V_{LCa}. In other words, the minimum amplitude of $V_{\mathrm{inva}LC}$ occurs when the compensation current I_{ca} is in phase with the voltage $V_{\mathrm{inva}LC}$. By further defining the power angle of I_{ca} as θ_{ca}, the mathematical relationship in (3) can be deduced from Fig. 7

$$V_{LCa}\left[V_{\mathrm{inva}LC\_\mathrm{min}}\right] = I_{ca}X_{LCa} = V_{ac}\left(\sin\theta_{ca}\right). \quad (3)$$

Varation of $V_{\text{inval}L}$ with coupled impedance and load power factor in RPC

(a)

Varation of $V_{\text{inval}LC}$ with coupled impedance and load power factor in HPQC
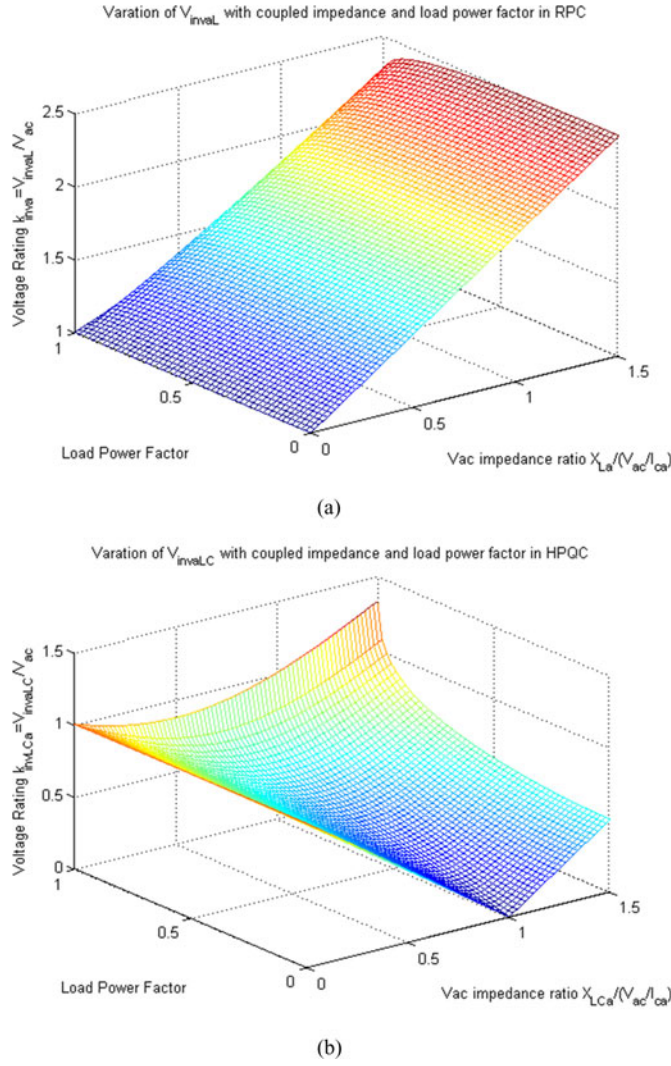
(b)

Fig. 5.   3-D plots showing the variation of voltage rating with V_{ac} phase coupled impedance under load PF in (a) RPC of the conventional structure and (b) HPQC of the proposed structure.

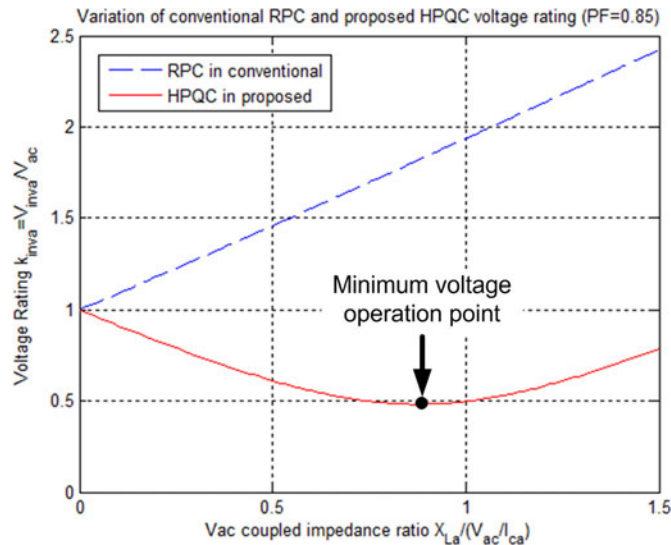Variation of conventional RPC and proposed HPQC voltage rating (PF=0.85)

Fig. 6.   Variation of voltage rating with V_{ac} phase coupled impedance in RPC of the conventional structure and in HPQC of the proposed structure.
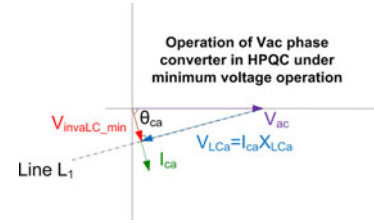

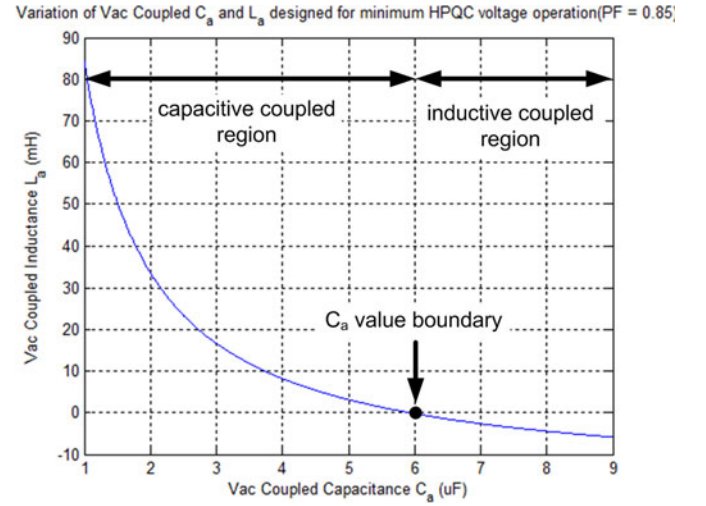Fig. 7.   Vector diagram showing the operation of V_{ac} phase.

Fig. 8.   Variation of L_a with C_a for minimum $V_{\text{inva}LC}$ (PF = 0.85, 15 MVA).

The corresponding V_{ac} coupled impedance X_{LCa} required for minimum $V_{\text{inva}LC}$ can, thus, be determined as shown in

$$X_{LCa}\left[V_{\text{inva}LC\_\min}\right] = \frac{V_{ac}\left(\sin\theta_{ca}\right)}{I_{ca}}. \tag{4}$$

With the aforementioned analysis, only the V_{ac} coupled impedance design for minimum HPQC voltage operation is determined. However, the ultimate goal of a parameter design is to determine the V_{ac} phase coupled inductance L_a and capacitance C_a for practical application. The linkage of X_{LCa} with C_a and L_a can be obtained through circuit analysis, as shown in

$$X_{LCa}\left[V_{\text{inva}LC\_\min}\right] = \frac{V_{ac}\left(\sin\theta_{ca}\right)}{I_{ca}} = -\left(\frac{\omega^2 L_a C_a - 1}{\omega C_a}\right). \tag{5}$$

For example, with V_{ac} of 27.5 kV, load PF of 0.85, and capacity of 15 MVA, the variation of L_a and C_a which satisfies the relationship in (5) is presented in Fig. 8. It can be observed that the relationship between L_a and C_a for minimum HPQC voltage rating is nonlinear. It is more practical for smaller physical size of lower inductance value. Furthermore, there is a limitation on the value of C_a, which is indicated by the large dot in Fig. 8. This is also the C_a value boundary. For a C_a value exceeding this boundary, the HPQC drops into the inductive coupled region, causing the operation similar to RPC. Minimum voltage operation in HPQC, thus, fails when the value of C_a is outside this boundary.
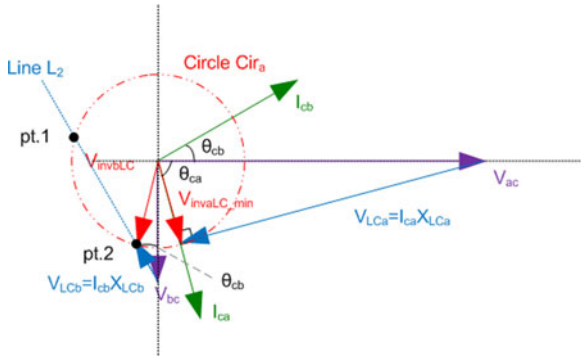
Fig. 9.   Vector diagram showing the operation of HPQC in correspondence with minimized $V_{\mathrm{inva}LC}$.

B. V_{bc} Phase Coupled Impedance Design

For the V_{bc} phase coupled impedance design, it is determined with matching to the minimum voltage $V_{\mathrm{inva}LC\_\min}$. The vector diagram showing the operation of V_{bc} phase converter in HPQC in correspondence with the $V_{\mathrm{inva}LC\_\min}$ is shown in Fig. 9. The minimum HPQC voltage is represented by the circle Cir_a with radius $V_{\mathrm{inva}LC\_\min}$. Assuming constant load PF and capacity, the vector V_{LCb} varies along the line L_2 with varying V_{bc} phase coupled impedance X_{LCb}. Two intersection points (pt.1 and pt.2) are present between the circle Cir_a and the line L_2. These two points are the operation points which satisfy the voltage matching with $V_{\mathrm{inva}LC\_\min}$. They may be determined mathematically.

The mathematical expression showing the intersection of circle Cir_a and the line L_2 is given in

$$V^2_{\mathrm{inva}LC\_\min} = (V^2_{LCb}\sin^2\theta_{cb} + (V_{bc} - V_{LCb}\cos\theta_{cb})^2). \quad (6)$$

By solving the expression, the mathematical expressions for pt.1 and pt.2 can be obtained in

$$(\text{pt.2})\frac{V_{bc}\cos\theta_{cb} - \sqrt{V^2_{\mathrm{inva}LC\_\min} - V^2_{bc}\sin^2\theta_{cb}}}{I_{cb}} = X_{LCb}$$

$$= \frac{V_{bc}\cos\theta_{cb} + \sqrt{V^2_{\mathrm{inva}LC\_\min} - V^2_{bc}\sin^2\theta_{cb}}}{I_{cb}}(\text{pt.1}) \quad (7)$$

Although both pt.1 and pt.2 may satisfy the voltage matching with $V_{\mathrm{inva}LC\_\min}$, operation point at pt.2 is preferred due to the lower impedance of X_{LCb} and lower power consumptions.

Besides the V_{bc} coupled impedance of X_{LCb}, there is another issue concerning about the value of V_{bc}. For the circle Cir_a to have intersections with the line L_2, the expression for X_{LCb} in (7) must be real values. Thus, the restrictions in (8) can thus be obtained

$$V_{bc} \le \frac{V_{\mathrm{inva}LC\_\min}}{\sin\theta_{cb}}. \quad (8)$$

C. Minimum HPQC Voltage Rating Achievable

After investigations of the V_{ac} and V_{bc} phase coupled impedance design for the minimum HPQC operation voltage,
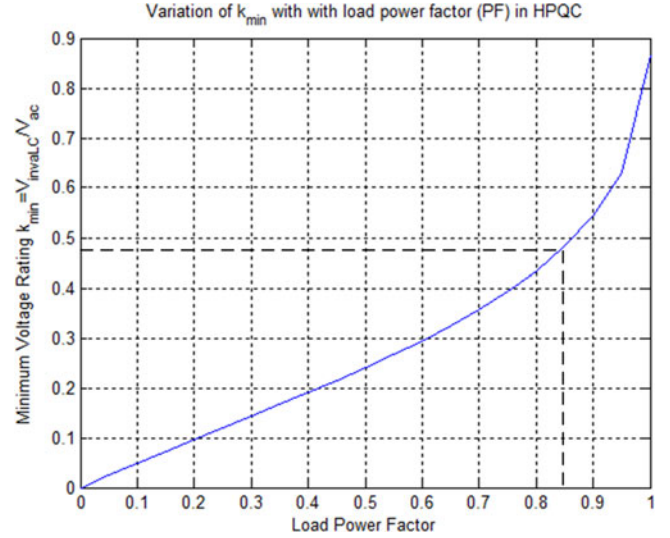

Fig. 10.   Curve showing the variation of HPQC minimum voltage rating (k_min) with load PF.

the minimum voltage rating achievable is discussed in this section.

The value of $V_{\mathrm{inva}LC\_\min}$ is a key factor in the minimum HPQC voltage rating achievable. By substituting the design of V_{ac} coupled impedance X_{LCa} in (4) into the HPQC $V_{\mathrm{inva}LC}$ voltage calculation in (2), the minimum value of $V_{\mathrm{inva}LC}$ in HPQC ($V_{\mathrm{inva}LC\_\min}$) can be obtained in

$$V_{\mathrm{inva}LC\_\min} = (\cos\theta_{ca})V_{ac}. \quad (9)$$

Neglecting the effect of V_{ac} phase voltage, the minimum HPQC voltage rating is determined by

$$k_{\min} = \frac{V_{\mathrm{inva}LC\_\min}}{V_{ac}} = \cos\theta_{ca}. \quad (10)$$

It is now obvious that the minimum HPQC voltage rating is dependent only on the power angle of I_{ca}. This again correlates with the load PF, as expressed in

$$\theta_{ca} = \tan^{-1}\left(\frac{\frac{1}{2\sqrt{3}}\mathrm{PF} + \sin(\cos^{-1}(\mathrm{PF}))}{\frac{1}{2}\mathrm{PF}}\right). \quad (11)$$

The curve showing the variation of minimum HPQC voltage rating ($k_{\min}$) against load PF is plotted in Fig. 10. It is equivalent to joining all the minimum operation points of the mesh plot in Fig. 5(b) under different load PF.

For example, with load PF of 0.85, the minimum voltage rating is approximately 0.48, which is consistent with the analysis in Section II. Assuming V_{ac} phase voltage of 27.5 kV, the minimum value of $V_{\mathrm{inva}LC}$ achievable is, thus, 13.2 kV. The peak value of the V_{ac} phase voltage is 38.89 kV, and the minimum HPQC dc-link voltage required is $\sqrt{2}$ times of $V_{\mathrm{inva}LC}$, which is approximately 18.67 kV.

IV. CONTROL PHILOSOPHY

The control block of the system is shown in Fig. 11.

The instantaneous load active and reactive power is computed using the modified instantaneous pq theory [25], [26]. The
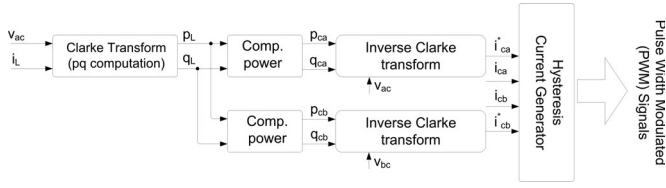
Fig. 11. Control block diagram of the HPQC for cophase traction power supply compensation.

mathematical expression is shown in (12), in which v_{ac} and i_L are the load voltage and current rms, while v_{acd} and i_{Ld} are 90° delay of load voltage and current, respectively. p_L and q_L refer to the instantaneous load active (real) and reactive (imaginary) power

$$\begin{bmatrix} p_L \\ q_L \end{bmatrix} = \begin{bmatrix} v_{ac} \cdot i_L + v_{acd} \cdot i_{Ld} \\ v_{acd} \cdot i_L - v_{ac} \cdot i_{Ld} \end{bmatrix}. \tag{12}$$

The active power part p_L can be split into dc part p_{dc} which corresponds to the fundamental average active load power; and oscillating part p_{ac} which corresponds to the oscillating active power between system source and load and contributes as part of harmonics and reactive power (which need to be compensated). The mathematical expression is shown in

$$p_L = p_{dc} + p_{ac}. \tag{13}$$

The required compensation power is then computed according to the power quality requirement, as expressed in (14), where p_{ca} and q_{ca} are the required active and reactive compensation power from the V_{ac} phase converter, while p_{cb} and q_{cb} are the required active and reactive compensation power from the V_{bc} phase converter

$$\begin{bmatrix} p_{ca} \\ q_{ca} \\ p_{cb} \\ q_{cb} \end{bmatrix} = \begin{bmatrix} \dfrac{1}{2} p_{dc} + p_{ac} \\ \dfrac{1}{2\sqrt{3}} p_{dc} + q \\ -\dfrac{1}{2} p_{dc} \\ -\dfrac{1}{2\sqrt{3}} p_{dc} \end{bmatrix}. \tag{14}$$

The reference of V_{ac} and V_{bc} phase compensation current, i_{ca}^* and i_{cb}^*, can then be computed according to (15) and (16), where v_{bc} and v_{bcd} are the V_{bc} phase voltage and its 90° delay value

$$i_{ca}^* = \frac{1}{v_{ac}^2 + v_{acd}^2} \begin{bmatrix} v_{ac} & v_{acd} \end{bmatrix} \begin{bmatrix} p_{ca} \\ q_{ca} \end{bmatrix} \tag{15}$$

$$i_{cb}^* = \frac{1}{v_{bc}^2 + v_{bcd}^2} \begin{bmatrix} v_{bc} & v_{bcd} \end{bmatrix} \begin{bmatrix} p_{cb} \\ q_{cb} \end{bmatrix}. \tag{16}$$

The computed reference current signal is then sent to the hysteresis current controller, which pulse width modulated signals are generated for the electronic switches of V_{ac} and V_{bc} phase converters.

The HPQC balances the grid-side current by transferring active power from the V_{ac} phase to the V_{bc} phase. Meanwhile,
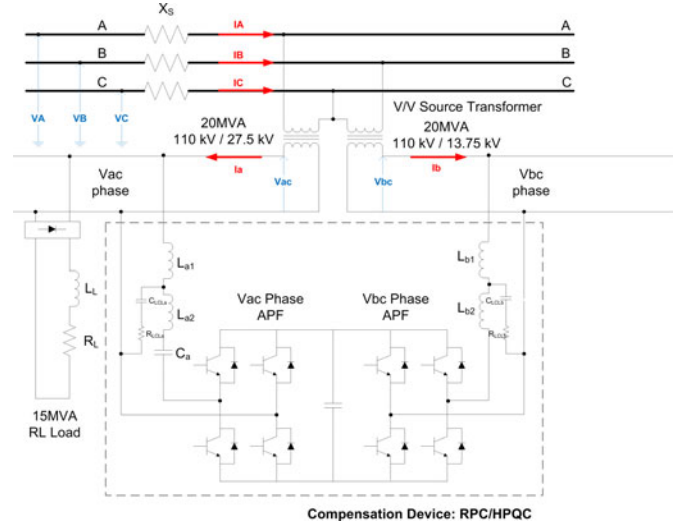

Fig. 12. Circuit schematic of the system under investigated in simulation verifications.

harmonic and reactive power compensations are achieved by the V_{ac} phase converter.

Concerning the design of the *LC* filter parameter, it is selected so as to reduce the harmonics compensation capacity of the compensator. Although the highest load harmonic contents are located at the third harmonic frequency, the *LC* filter is tuned at the second highest load harmonics (fifth harmonic) for smaller physical size of the components.

V. SIMULATION VERIFICATIONS

Simulations using PSCAD/EMTDC are done to verify the aforementioned theoretical studies. The circuit schematic of the system used in simulations is provided in Fig. 12.

The parameters are selected as close to practical applications as possible [16], [19], [27]. The substation V/V transformer is composed of two 20 MVA single-phase transformers, with turning ratios of 110 kV/27.5 kV and 110 kV/13.75 kV. Traction loads are simulated using rectifier *RL* load, with linear capacity of 15 MVA. The compensation device is then connected across the two single-phase outputs of V/V transformer to provide power quality compensation of the system. Notice that the *LCL* filter is included here to filter the ripples introduced by the compensator.

A. Cophase Traction Power Without Compensation

The system performance without compensation is investigated first. Shown in Fig. 13 are the three-phase source, secondary voltage, and current waveforms for cophase traction power without compensation. It could be observed that the system suffers from unbalance, reactive power and harmonics problem.
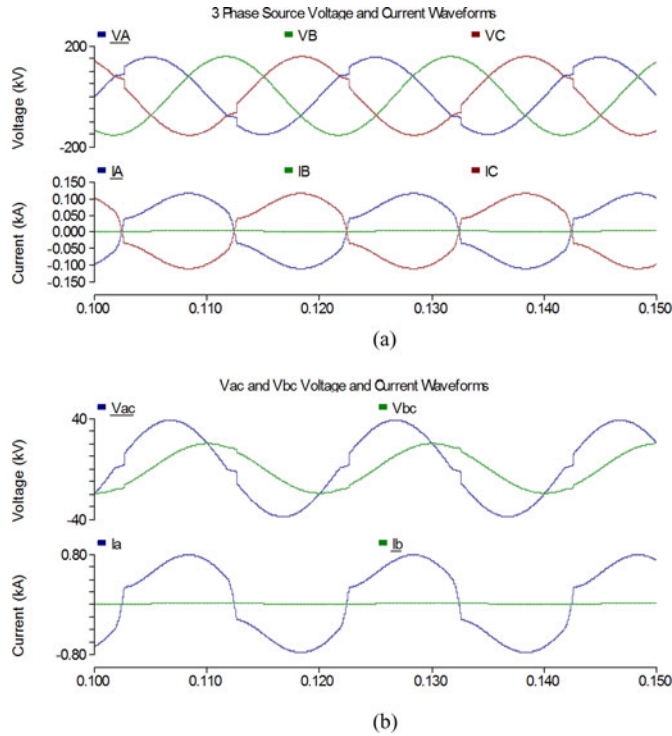
Fig. 13.   System performances of the proposed cophase traction power without compensation. (a) Three-phase power source voltage and current waveforms. (b) V_{ac} and V_{bc} phase voltage and current waveforms.

TABLE I
RPC CIRCUIT PARAMETERS USED IN THE SIMULATION VERIFICATIONS

No.	Items	Description
1	Vac Coupling Inductance 1 L_{a1}	3.4 mH
2	Vac Coupling Inductance 2 L_{a2}	3.4 mH
3	Vac LCL Capacitance C_{LCLa}	5 uF
4	Vac LCL Damped Resistance R_{LCLa}	20 ohm
5	DC Link Capacitance C_{dc}	10000 uF
6	Vbc Coupling Inductance 1 L_{b1}	4 mH
7	Vbc Coupling Inductance 2 L_{b2}	4 mH
8	Vbc LCL Capacitance C_{LCLb}	5.63 uF
9	Vbc LCL Damped Resistance R_{LCLb}	20 ohm

B. Cophase Traction Power With Conventional RPC ($V_{dc} = 41$ kV)

Next, simulation verifications are performed on cophase traction power with RPC to investigate the compensation performance. The RPC circuit parameters are shown in Table I. Besides C_a, the other values are chosen according to the parameter design in Section III. The dc-link voltage is selected slightly higher than the peak voltage of V_{ac} phase, as required by the design of RPC. The simulated system performances are shown in Fig. 13. It can be observed that the system power quality problems such as unbalance and harmonics are compensated.

TABLE II
HPQC CIRCUIT PARAMETERS USED IN THE SIMULATION VERIFICATIONS

| No.	Items	Description
1	Vac Coupling Inductance 1 L_{a1}	3.4 mH
2	Vac Coupling Inductance 2 L_{a2}	3.4 mH
3	Vac Coupling Capacitance C_a	60 uF
4	Vac LCL Capacitance C_{LCLa}	5 uF
5	Vac LCL Damped Resistance R_{LCLa}	20 ohm
6	DC Link Capacitance C_{dc}	10000 uF
7	Vbc Coupling Inductance 1 L_{b1}	4 mH
8	Vbc Coupling Inductance 2 L_{b2}	4 mH
9	Vbc LCL Capacitance C_{LCLb}	5.63 uF
10	Vbc LCL Damped Resistance R_{LCLb}	20 ohm
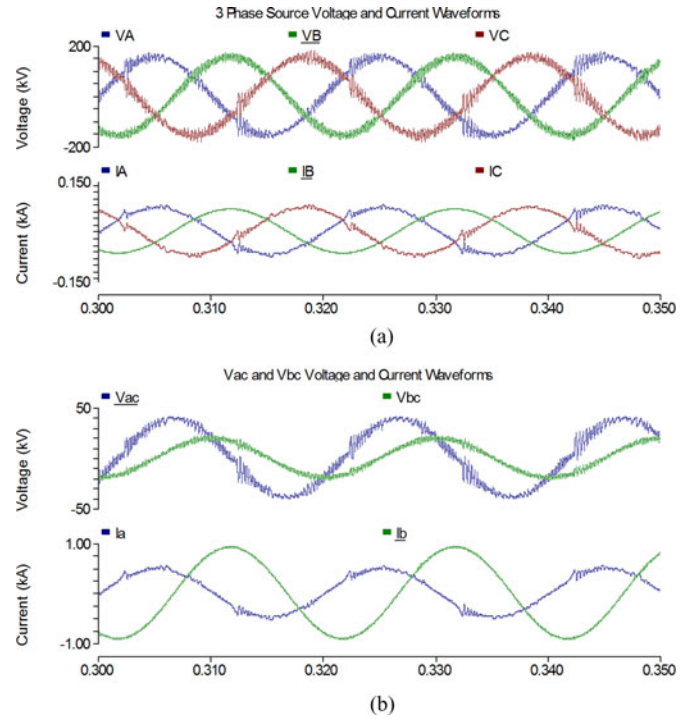
Fig. 14.   System performances of cophase traction power with RPC ($V_{dc} = 41$ kV). (a) Three-phase power source voltage and current waveforms. (b) V_{ac} and V_{bc} phase voltage and current waveforms.

C. Cophase Traction Power With Proposed HPQC ($V_{dc} = 27$ kV)

Afterward, simulations verifications are also performed on the proposed cophase traction power with HPQC. The HPQC circuit parameters used in the simulations are presented in Table II. They are all designed and selected based on the discussions for minimum HPQC voltage operation. Since the load harmonic contents are mostly concentrated at the third and fifth fundamental frequencies, for lower harmonic compensation capacity, the values of coupling inductance and capacitance are chosen at fifth harmonics (for lower impedance and smaller component size). The simulated load PF is around 0.94. According to the investigations, the minimum HPQC voltage rating k_{min} is 0.61. With traction load electrified by 27.5 kV, the minimum value of
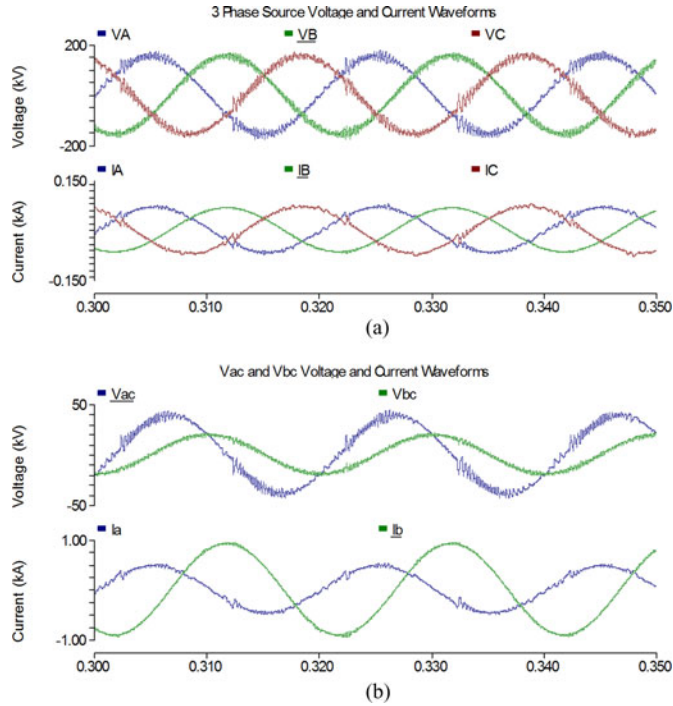
Fig. 15. System performances of the proposed cophase traction power supply system with HPQC ($V_{dc} = 27$ kV). (a) Three-phase power source voltage and current waveforms. (b) V_{ac} and V_{bc} phase voltage and current waveforms.

TABLE III
SUMMARIZED SYSTEM STATISTICS IN SIMULATION

	Three Phase Source								
	Without Compensation			With compensation using RPC (V_{dc}=41 kV)			With compensation using HPQC (V_{dc}=27 kV)		
	A	B	C	A	B	C	A	B	C
Current rms (A)	81.13	0.00	81.13	52.08	48.19	53.27	49.00	48.21	51.66
Current THD (%)	12.95	---	12.95	4.58	0.42	4.43	3.12	0.79	2.74
Power Factor	0.57	0.87	0.99	0.99	0.99	0.99	0.99	0.99	0.99
Current Unbalance (%)	99			3.95			5.57		

$V_{\mathrm{inva}LC}$ in HPQC is 16.78 kV. The dc-link voltage of HPQC used in the simulation is 27 kV.

The simulated system waveforms are shown in Fig. 15. Comparing them with the results obtained using RPC in Fig. 14, it can be observed that the compensation performance of HPQC in cophase traction power is more or less the same. For further investigations of the system performance, the simulated system statistics of cophase traction power without compensation, with RPC, and with HPQC are summarized in Table III. It can be observed that with similar compensation performance, the minimum HPQC operation voltage is only 66% of that in RPC. This shows a great advantage of HPQC operation at minimum voltage over RPC.

D. Cophase Traction Power With Proposed HPQC ($V_{dc} = 24.3, 27, and 29.7$ kV)

In order to investigate the compensation performances of the proposed HPQC around the dc-link voltage of 27 kV, simulations are done with proposed HPQC at 0.9 (24.3 kV) and 1.1 (29.7 kV) of 27 kV. The simulation results obtained are pre-

TABLE IV
SIMULATED COMPENSATION PERFORMANCE OF THE PROPOSED HPQC AT 24.3, 27, AND 29.7 KV.

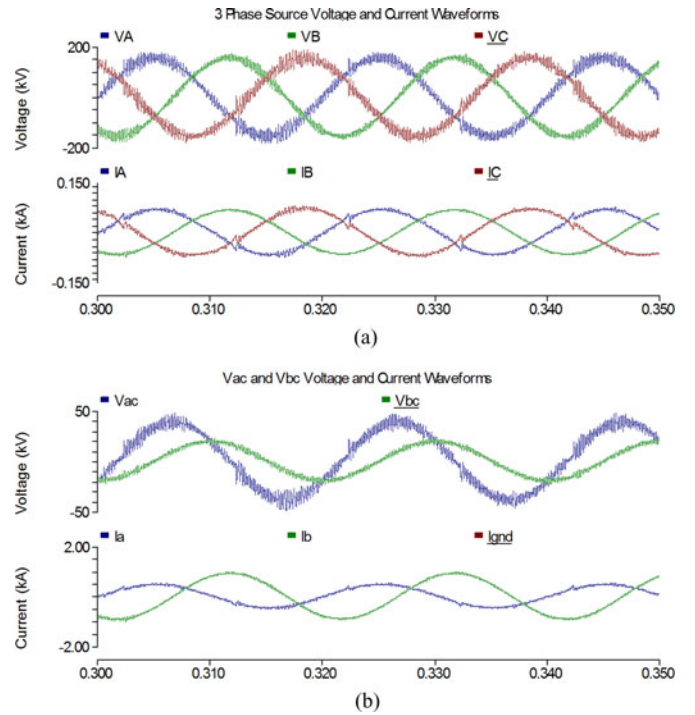|	Three Phase Source								
	With compensation using HPQC (V_{dc}=24.3 kV)			With compensation using HPQC (V_{dc}=27 kV)			With compensation using HPQC (V_{dc}=29.7 kV)		
	A	B	C	A	B	C	A	B	C
Current rms (A)	59.27	47.12	67.20	49.00	48.21	51.66	48.33	47.74	50.39
Current THD (%)	23.32	0.98	20.93	3.12	0.79	2.74	5.02	0.88	4.86
Power Factor	0.96	0.99	0.99	0.99	0.99	0.99	0.99	0.99	0.99
Current Unbalance (%)	19.07			5.57			4.42		

Fig. 16. System performances of the proposed cophase traction power supply system with HPQC ($V_{dc} = 41$ kV). (a) Three-phase power source voltage and current waveforms. (b) V_{ac} and V_{bc} phase voltage and current waveforms.

sented in Table IV. It can be observed that with dc-link voltage lower than 27 kV in the proposed HPQC, the compensation performances become worse. The source current THD and unbalance are both above standard. On the other hand, when the dc-link voltage is above 27 kV, the compensation performance is more or less the same as that using 27 kV. It may thus be concluded that under the simulated conditions, the optimum dc-link voltage of the proposed HPQC is 27 kV.

E. Cophase Traction Power With Proposed HPQC ($V_{dc} = 41$ kV)

There may be wonder whether the compensation performance can be enhanced with higher dc-link voltage; simulations are thus performed with proposed HPQC at dc-link voltage of 41 kV (voltage level of conventional RPC) for comparisons. The waveforms captured are shown in Fig. 16. It can be observed that the proposed HPQC at 41 kV is able to compensate system unbalance, reactive power, and harmonics. Comparing Fig. 16 with Fig. 15, it can be seen that the compensation performance is

TABLE V
SUMMARIZED SYSTEM STATISTICS IN SIMULATION

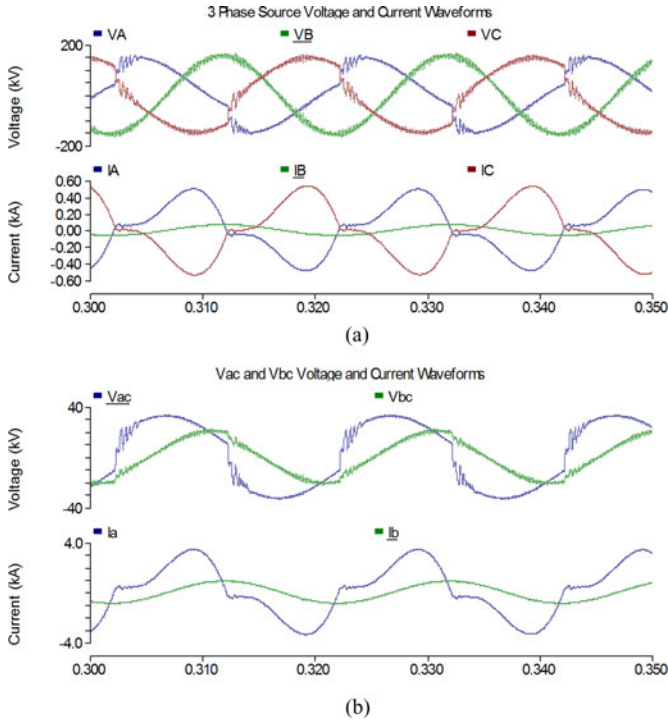| | Three Phase Source | | | | | |
| | With compensation using RPC (V_{dc}=41 kV) | | | With compensation using HPQC (V_{dc}=41 kV) | | |
	A	B	C	A	B	C
Current rms (A)	52.08	48.19	53.27	47.63	47.46	49.91
Current THD (%)	4.58	0.42	4.43	4.18	0.68	3.97
Power Factor	0.99	0.99	0.99	0.99	0.99	0.99
Current Unbalance (%)	3.95			4.12		

Fig. 17. System performances of the cophase traction power supply system with RPC (V_{dc} = 27 kV). (a) Three-phase power source voltage and current waveforms. (b) V_{ac} and V_{bc} phase voltage and current waveforms.

similar but the voltage ripples introduced are larger due to the higher dc-link voltage level. Summarization of system performances using the conventional RPC and the proposed HPQC at dc-link voltage of 41 kV is presented in Table V. Comparing the data with the performances of the proposed HPQC at 27 kV is shown in Table III. The compensation performance is more or less the same, but the dc-link voltage level used is lower.

F. Cophase Traction Power With Conventional RPC (V_{dc} = 27 kV)

Besides the aforementioned simulation verifications, simulations are also performed on cophase traction power with RPC operating at minimum HPQC voltage. The circuit parameters are selected as shown in Table I. The dc-link voltage is chosen as the minimum HPQC operation voltage (V_{dc} = 27 kV). The simulated system waveforms are shown in Fig. 17. It can be observed that unlike HPQC, the compensation performance of RPC at the minimum HPQC voltage operation point is far from
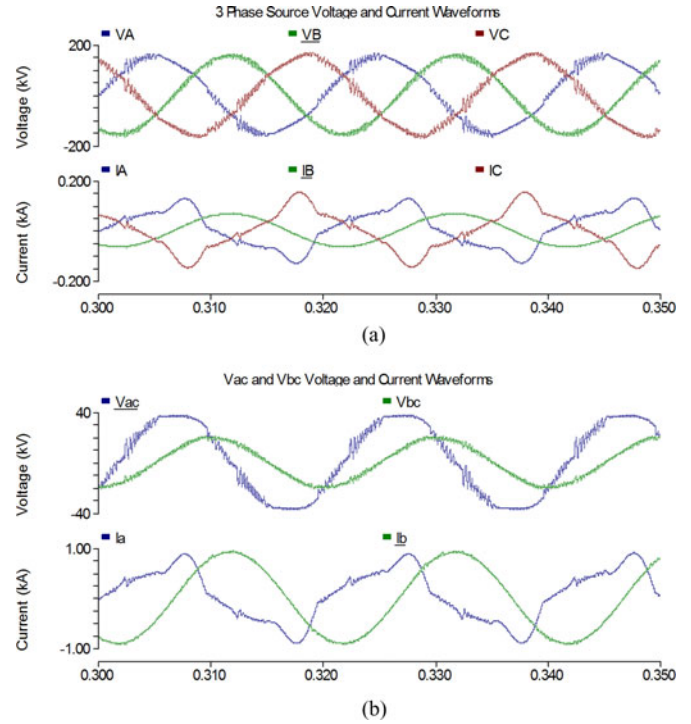

Fig. 18. System performances of the proposed cophase traction power supply system with HPQC (V_{dc} = 22 kV). (a) Three-phase power source voltage and current waveforms. (b) V_{ac} and V_{bc} phase voltage and current waveforms.

TABLE VI
SUMMARIZED SYSTEM STATISTICS IN COPHASE TRACTION POWER WITH
HPQC UNDER OPERATION VOLTAGE BELOW MINIMUM (V_{dc} = 22 kV) AND AT
MINIMUM (V_{dc} = 27 kV)

| | Three Phase Source | | | | | |
| | With compensation using HPQC (V_{dc}=22 kV) | | | After compensation using HPQC (V_{dc}=27 kV) | | |
	A	B	C	A	B	C
Current rms (A)	74.05	47.42	79.88	49.00	48.21	51.66
Current THD (%)	32.67	1.34	30.43	3.12	0.79	2.74
Power Factor	0.95	0.99	0.99	0.99	0.99	0.99
Current Unbalance (%)	26.89			5.57		

satisfactory. This shows the great advantage of reduced voltage operation in HPQC over RPC.

G. Cophase Traction Power With Proposed HPQC (V_{dc} = 22 kV)

Finally, simulations are performed on cophase traction power with HPQC operating below the minimum operation voltage. The circuit parameters are shown in Table II and the dc-link voltage is reduced to 22 kV (chosen as 80% of the optimum dc-link voltage level 27 kV). The simulated system waveforms under such conditions are presented in Fig. 18. It can be observed that the compensation performance of HPQC below the minimum operation voltage is far from satisfactory. This shows that the minimum operation voltage rating derived in Section III-C is valid for HPQC in the cophase traction power supply system.
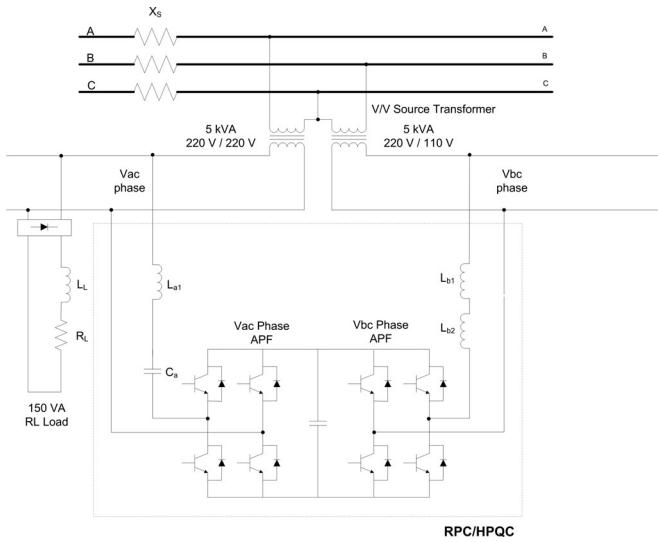
Fig. 19. Circuit schematic of the hardware prototype for verification of performances in the proposed cophase traction power supply system with HPQC.
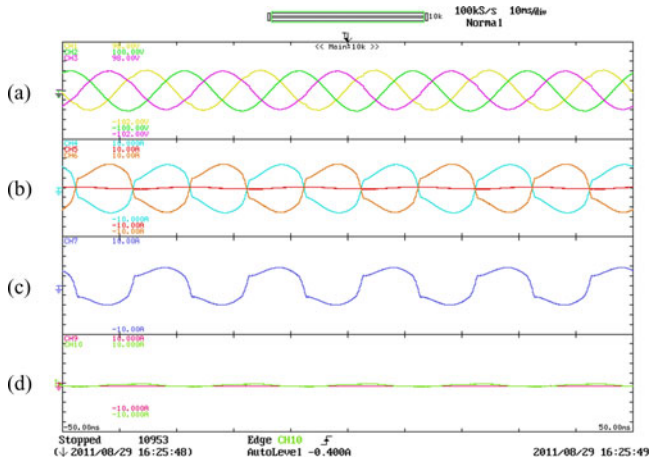

Fig. 20. System waveforms for cophase traction power supply without compensation: (a) three-phase source voltage, (b) three-phase source current, (c) load current, and (d) V_{ac} and V_{bc} phase compensation current.

TABLE VII
RPC CIRCUIT PARAMETERS IN HARDWARE PROTOTYPE

No.	Items	Description
1	Vac Coupling Inductance 1 La$_1$	2 mH
2	DC Link Capacitance C$_{dc}$	5000 uF
3	Vbc Coupling Inductance 1 Lb$_1$	2 mH
4	Vbc Coupling Inductance 2 Lb$_2$	9 mH
5	Load Inductance L$_L$	30 mH
6	Load Resistance R$_L$	10 ohm

The summarized statistics of cophase traction power with HPQC operation voltage below and at minimum value are compared in Table VI. It can be observed that when the HPQC operation voltage is below the minimum value, the compensation performance is far from satisfactory.
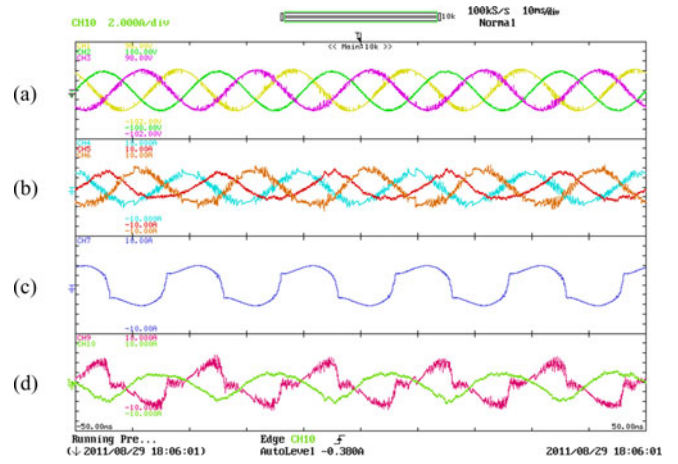

Fig. 21. System waveforms for cophase traction power supply with RPC compensation (V_{dc} = 76 V): (a) three-phase source voltage, (b) three-phase source current, (c) load current, and (d) V_{ac} and V_{bc} phase compensation current.

TABLE VIII
HPQC CIRCUIT PARAMETERS IN HARDWARE PROTOTYPE

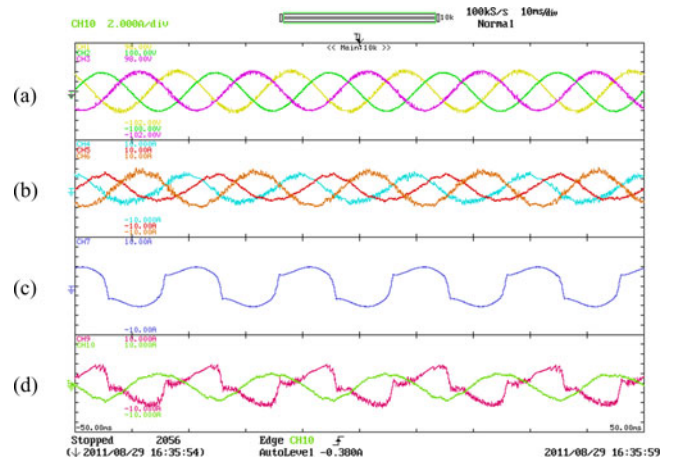| No.	Items	Description
1	Vac Coupling Capacitance C$_a$	220 uF
2	Vac Coupling Inductance 1 La$_1$	2 mH

Fig. 22. System waveforms for cophase traction power supply with minimum HPQC voltage operation: (a) three-phase source voltage, (b) three-phase source current, (c) load current, (d) V_{ac} and V_{bc} phase compensation current.

VI. EXPERIMENTAL RESULTS

In order to verify the system performances of the proposed cophase traction power supply system with HPQC of minimum operation voltage, a low-capacity laboratory-scaled hardware prototype is constructed. The circuit schematic of the prototype is shown in Fig. 19.

Notice that the *LCL* filter can be omitted here since it is a low-voltage application. The V/V transformer is composed of two 5-kVA single-phase transformers. The traction load is represented using rectifier *RL* circuit, with linear capacity of 150 VA. The operation voltage of V_{ac} is 50 V, which is 540 times scaled down from the simulation settings. According to this scale, the

TABLE IX
COMPARISONS OF SYSTEM COMPENSATION PERFORMANCE

	Three Phase Source								
	Without Compensation			With RPC compensation (V_{dc} = 76V)			With HPQC compensation (V_{dc} = 52V)		
	A	B	C	A	B	C	A	B	C
Current rms (A)	3.47	0.11	3.79	2.03	1.76	2.50	1.81	1.76	2.50
Current THD (%)	19.0	---*	17.6	8.3	9.4	10.6	9.7	8.8	3.7
Power Factor	0.61	---*	1.00	0.97	1.00	1.00	0.96	1.00	0.99

* Unavailable due to absence of phase B current without compensation

required dc-link voltage for the conventional RPC is 76 V and the minimum dc-link voltage achievable for the proposed HPQC is around 50 V.

A. Cophase Traction Power Without Compensation

First, the system performance of cophase traction power without compensation is investigated. The system waveforms obtained are shown in Fig. 20. It can be clearly observed that the system suffers from unbalance and harmonic problem.

B. Cophase Traction Power With RPC Compensation (V_{dc} = 76 V)

Next, experiments are conducted on cophase traction power with RPC compensation. The dc-link voltage is set as 76 V, according to the scaled down value from the simulations. The RPC circuit parameters used in the hardware prototype are shown in Table VII. With system voltage of 50 V, the peak voltage is around 70.71 V, and the dc-link voltage used in RPC is 76 V. The system waveforms obtained with RPC under such conditions are presented in Fig. 21. It can be observed that three-phase source current becomes balanced, and harmonics are eliminated.

C. Cophase Traction Power With Proposed HPQC Compensation (V_{dc} = 52 V)

Afterward, experimental results are presented with cophase traction power supply with HPQC compensation. The V_{ac} coupling impedance is provided in Table VIII and all the other main circuit parameters are the same as those in Table V. They are all selected according to the design procedure proposed in this paper. Experiments are done on 50-V voltage level. With peak voltage of 70.71 V, the dc-link voltage of HPQC used is 52 V.

The system waveforms obtained through experimental results are shown in Fig. 22. It can be observed that with HPQC operating at minimum voltage, the system unbalance, reactive power, and harmonics are compensated. It can be concluded that HPQC can provide similar compensation performance as RPC with a lower and minimum dc-link voltage.

For comparisons, summarized data of system statistics without compensation, with RPC compensation (V_{dc} = 76 V), and with HPQC compensation (V_{dc} = 52 V) are shown in Table IX. There is a 30% decrease in dc-link voltage in HPQC for similar
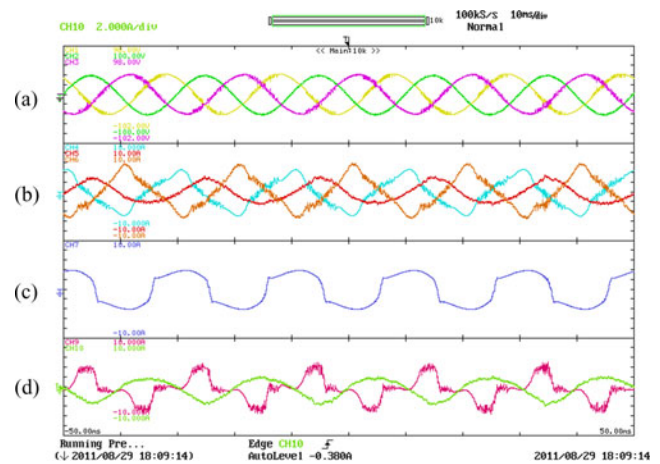

Fig. 23. System waveforms for cophase traction power supply with RPC compensation (V_{dc} = 52 V): (a) three-phase source voltage, (b) three-phase source current, (c) load current, (d) V_{ac} and V_{bc} phase compensation current.

compensation performance as RPC. The experimental results with compensation are all satisfied with the IEEE standard for power quality [5].

D. Cophase Traction Power With Conventional RPC (V_{dc} = 52 V)

Finally, experiments are conducted using cophase traction power with RPC at a dc-link voltage of 52 V. This is also the minimum operation voltage achievable using HPQC. The system waveforms obtained are shown in Fig. 23.

It can be observed that with dc-link voltage of 52 V, the compensation performance provided by RPC in cophase traction is far from satisfactory. For reference, the comparisons of system performance in cophase traction power without compensation, with compensation using RPC and HPQC (V_{dc} = 52 V) are summarized in Table X. It can be observed that with the minimum dc-link voltage level achievable using HPQC, satisfactory compensation performance cannot be provided by RPC.

It can be observed from the experimental results that with load PF of 0.94, the dc-link voltage of the cophase traction power supply power quality compensator can be reduced to 68% of that in conventional RPC with proposed HPQC. While providing the same output compensation current and

TABLE X
COMPARISONS OF SYSTEM COMPENSATION, WITH RPC (V_{dc} = 52 V) AND WITH PROPOSED HPQC (V_{dc} = 52 V)

	Three Phase Source								
	Without Compensation			With RPC compensation (V_{dc} = 52V)			With HPQC compensation (V_{dc} = 52V)		
	A	B	C	A	B	C	A	B	C
Current rms (A)	3.47	0.11	3.79	2.71	1.74	3.21	1.81	1.76	2.50
Current THD (%)	19.0	---*	17.6	21.2	16.9	18.7	9.7	8.8	3.7
Power Factor	0.61	---*	1.00	0.95	1.00	1.00	0.96	1.00	0.99

* Unavailable due to absence of phase B current without compensation

similar compensation performance, the device capacity of the proposed HPQC is reduced by 32% compared to conventional RPC. Reduction of dc-link operation voltage rating can in another sense reduce the power consumptions. As discussed in the first section, the average cost of active compensation device is around USD $60/kVA, while that of passive compensation device is only approximately $5/kVA. Concerning the V_{ac} phase converter alone, for conventional 5 MVA RPC, the installation cost is estimated to be USD $300 000. However, with proposed HPQC, the capacity is only 3.4 MVA, which leads to an estimation of USD $221 000 (73% of that in conventional RPC).

VII. CONCLUSION

A HPQC with reduced dc voltage operation compared to conventional RPC during compensation is proposed in this paper. The parameter design for the minimum HPQC voltage operation is being discussed, and the minimum HPQC voltage operation point achievable is explored. It is found that the minimum HPQC operation voltage rating is dependent only on the traction load PF. It increases with increasing load PF. For instance, with load PF of 0.85, the minimum HPQC voltage rating is only 0.48. It is also verified through simulation that the HPQC would operate at the minimum voltage with the proposed parameter design, and the voltage operation point is lower than that of conventional RPC. It is also shown through experimental results of the hardware prototype that the operation voltage of HPQC is only 70% of the conventional RPC.

REFERENCES

[1] P. E. Sutherland, M. Waclawiak, and M. F. McGranaghan, "System impacts evaluation of a single-phase traction load on a 115-kV transmission system," *IEEE Trans. Power Delivery*, vol. 21, no. 2, pp. 837–844, Apr. 2006.

[2] H. Y. Kuo and T. H. Chen, "Rigorous evaluation of the voltage unbalance due to high-speed railway demands," *IEEE Trans. Veh. Technol.*, vol. 47, no. 4, pp. 1385–1389, Nov. 1998.

[3] D. C. Howroyd, "Public-supply-system distortion and unbalance from single-phase a.c. traction," *Proc. Inst. Electr. Eng.*, vol. 124, no. 10, pp. 853–859, 1977.

[4] *IEEE Recommended Practice for Monitoring Electric Power Quality,* IEEE Standard 1159-1995.

[5] *IEEE Recommended Practices and Requirements for Harmonic Control in Electrical Power Systems* IEEE Standard 519-1992.

[6] S. T. Senini and P. J. Wolfs, "Novel topology for correction of unbalanced load in single phase electric traction systems," in *Proc. IEEE 33rd Annu. Power Electron. Spec. Conf.*, Jun. 2002, vol. 3, pp. 1208–1212.

[7] Z. Zhang, B. Wu, J. Kang, and L. Luo, "A multi-purpose balanced transformer for railway traction applications," *IEEE Trans. Power Delivery*, vol. 24, no. 2, pp. 711–718, Apr. 2009.

[8] H. Wang, Y. Tian, and Q. Gui, "Evaluation of negative sequence current injection into the public grid from different traction substation in electrical railways," in *Proc. 20th Int. Conf. Exhib. Electr. Distrib.—Part 1*, 2009, pp. 1–4.

[9] C. Dai and Y. Sun, "Investigation of the imbalance current compensation for transformers used in electric railways," in *Proc. Asia-Pacific Power Energy Eng. Conf.*, 2010, pp. 1–4.

[10] Z. Sun, X. Jiang, D. Zhu, and G. Zhang, "A novel active power quality compensator topology for electrified railway," *IEEE Trans. Power Electron.*, vol. 19, no. 4, pp. 1036–1042, Jul. 2004.

[11] P. C. Tan, R. E. Morrison, and D. G. Holmes, "Voltage form factor control and reactive power compensation in a 25-kV electrified railway system using a shunt active filter based on voltage detection," *IEEE Trans. Ind. Appl.*, vol. 39, no. 2, pp. 575–581, Mar./Apr. 2003.

[12] Z. Shu, S. Xie, and Q. Z. Li, "Development and implementation of a prototype for co-phase traction power supply system," in *Proc. Asia-Pacific Power Energy Eng. Conf.*, 2010, pp. 1–4.

[13] M. Chen, Q. Li, and G. Wei, "Optimized design and performance evaluation of new cophase traction power supply system," in *Proc. Asia-Pacific Power Energy Eng. Conf.*, 2009, pp. 1–6.

[14] G. Zeng and R. Hao, "Analysis and design of an active power filter for three-phase balanced electrified railway power supply system," in *Proc. 5th Int. Conf. Power Electron. Drive Syst.*, 2003, vol. 2, pp. 1510–1513.

[15] F. Zhou, Q. Li, and D. Qiu, "Co-phased traction power system based on balanced transformer and hybrid compensation," in *Proc. Asia-Pacific Power Energy Eng. Conf.*, 2009, pp. 1–4.

[16] A. Luo, C. Wu, J. Shen, Z. Shuai, and F. Ma, "Railway static power conditioners for high-speed train traction power supply systems using three-phase V/V transformers," *IEEE Trans. Power Electron.*, vol. 26, no. 10, pp. 2844–2856, Oct. 2011.

[17] A. Luo, F. Ma, C. Wu, S. Q. Ding, Q.-C. Zhong, and Z. Shuai, "A dual-loop control strategy of railway static power regulator under V/V electric traction system," *IEEE Trans. Power Electron.*, vol. 26, no. 7, pp. 2079–2091, Jul. 2011.

[18] Z. Shu, S. Xie, and Q. Li, "Single-phase back-to-back converter for active power balancing, reactive power compensation, and harmonic filtering in traction power system," *IEEE Trans. Power Electron.*, vol. 26, no. 2, pp. 334–343, Feb. 2011.

[19] W. Y. Dong, "Research on control of comprehensive compensation for traction substations based on the STATCOM technology," Ph.D. dissertation, Tsinghua Univ., Beijing, China, 2009.

[20] V. , B. Corasaniti, M. B. Barbieri, P. L. Arnera, and M. I. Valla, "Hybrid active filter for reactive and harmonics compensation in distribution network," *IEEE Trans. Ind. Electron.*, vol. 56, no. 3, pp. 670–677, Mar. 2009.

[21] H. Akagi and K. Isozaki, "A hybrid active filter for a three-phase 12-pulse diode rectifier used as the front end of a medium-voltage motor drive," *IEEE Trans. Power Electron.*, vol. 27, no. 1, pp. 69–77, Jan. 2012.

[22] Z. Shuai, A. Luo, J. Shen, and X. Wang, "Double closed-loop control method for injection-type hybrid active power filter," *IEEE Trans. Power Electron.*, vol. 26, no. 9, pp. 2393–2403, Sep. 2011.

[23] M. K. Sahu and G. Poddar, "Transformerless hybrid topology for medium-voltage reactive-power compensation," *IEEE Trans. Power Electron.*, vol. 26, no. 5, pp. 1469–1479, May 2011.

[24] J. Ma, M. Wu, and S. Yang, "The application of SVC for the power quality control of electric railways," in *Proc. Int. Conf. Sustainable Power Gener. Supply*, 2009, pp. 1–5.

[25] E. H. Watanabe, M. Aredes, J. L. Afonso, J. G. Pinto, L. F. C. Monteiro, and H. Akagi, "Instantaneous p–q power theory for control of compensators in micro-grids," in *Proc. Int. School on Nonsinusoidal Curr. Compensation*, 2010, pp. 17–26.

[26] E. H. Watanabe, H. Akagi, and M. Aredes, "Instantaneous p-q power theory for compensating nonsinusoidal systems," in *Proc. Int. School onNonsinusoidal Curr. Compensation*, 2008, pp. 1–10.

[27] L. Battistelli, M. Pagano, and D. Proto, "2× 25-kV 50 Hz high-speed traction power system: Short-circuit modeling," *IEEE Trans. Power Delivery*, vol. 26, no. 3, pp. 1459–1466, Jul. 2011.

Wei-Gang Liu received the B.Sc. degree (highest Hons.) in electronic and information engineering from JiLin University, ChangChun, China, in 2004. He has been studying the M.Sc. degree in the Department of Electrical and Electronics Engineering, University of Macau (UM), Macao, China, since 2008.

He is currently a Master Research Fellow in the Power Electronics Laboratory, Faculty of Science and Technology, UM. His research interests include electrified railway, fuzzy control, and neural network. He has published one conference paper in the field of interests.

Keng-Weng Lao received the B.Sc. and M.Sc. degrees in electrical and electronics engineering from the Faculty of Science and Technology, University of Macau, Macau, China, in 2009 and 2011, respectively. He is currently working toward the Ph.D. degree at the Department of Electrical and Computer Engineering, University of Macau.

His research interests include FACTS and compensation devices, power quality, energy saving, and renewable energy.

Mr. Lao received the Champion Award of the "Schneider Electric Energy Efficiency Cup 2010" in Hong Kong.

Man-Chung Wong (SM'06) received the B.Sc. and M.Sc. degrees in electrical and electronics engineering from the Faculty of Science and Technology, University of Macau, Macau, China, in 1993 and 1997, respectively, and the Ph.D. degree from the Tsinghua University, Beijing, China, in 2003.

He has been an Associate Professor at the University of Macau since 2008. His research interests include flexible alternating current transmission system and distributed flexible alternating current transmission system, power quality, custom power, and pulsewidth modulation. .

Dr. Wong received the Young Scientist Award from the "Instituto Internacional De Macau" in 2000, the Young Scholar Award from the University of Macau in 2001, and the second prize of 2003 Tsinghua University Excellent Ph.D. thesis award.

NingYi Dai (M'05) was born in Jiangsu, China, in 1979. She received the B.Sc. degree in electrical engineering from the Southeast University, Nanjing, China, in 2001, and the M.Sc. and Ph.D. degrees in electrical and electronics engineering from the Faculty of Science and Technology, University of Macau, Macao, China, in 2004 and 2007, respectively.

She is currently an Assistant Professor in the Department of Electrical and Computer Engineering, University of Macau. She has published more than ten technical journals and conference papers in the field of power system and power electronics. Her research interests include application of power electronics in power system, power conversion technology, and pulsewidth modulation.